11D.2

THE INFLUENCE OF THE MJO ON UPSTREAM PRECURSORS TO AFRICAN EASTERLY WAVES

Ghassan J. Alaka Jr. * and Eric. D. Maloney
Colorado State University, Fort Collins, Colorado

1. INTRODUCTION

African easterly waves (AEWs) are synoptic-scale disturbances that initiate near the African easterly jet (AEJ) and propagate into the Atlantic. Since AEWs seed tropical cyclones, a better understanding of how wave activity in West Africa varies on intraseasonal timescales could help predict periods of increased or decreased cyclogenesis in the Atlantic. Recent work suggests that the MJO may have a significant remote influence on North Africa during boreal summer, including a modulation of the West African monsoon (e.g. Matthews 2004; Janicot et al. 2009; Leroux and Hall 2009). These studies have shown that increased convection in the West African monsoon coincides with MJO convective initiation over the Indian Ocean. It is hypothesized that Kelvin and Rossby waves, while traveling in opposite zonal directions, force variability in the West African monsoon region at approximately the same time (Matthews 2004; Janicot et al. 2009). Understanding how and why the MJO impacts West African wave activity may have a profound influence on Atlantic tropical cyclone prediction due to the predictability of the MJO.

This study aims to identify how the MJO induces convection and AEW variability east of Lake Chad. Carlson (1969) first proposed the importance of convection associated with topographical features east of ~10°E to AEW initiation. More recent studies hypothesized that upstream convection, in an East African region including the Darfur Mountains (15°N, 23°E) and the Ethiopian Highlands (10°N, 35°E), initiates AEWs near the entrance of the AEJ (Hall et al. 2006; Thorncroft et al. 2008; Leroux and Hall 2009).

In a modeling study, Thorncroft et al. (2008) used a primitive equation model to analyze how effective different heating profiles (shallow, deep, stratiform) and their horizontal locations are at initiating AEW variability when given a common basic state AEJ. When heating profiles were applied at (15°N, 20°E), which is in the Darfur region near the AEJ entrance, strong divergence anomalies near the AEJ level produced high amplitude wave disturbances downstream, particularly when using shallow convection and stratiform heating profiles.

* *Corresponding author address:* Ghassan J. Alaka Jr., Dept. of Atmospheric Science, Colorado State University, 1371 Campus Delivery, Fort Collins, CO 80523-1371; e-mail: gusalaka@atmos.colostate.edu.

Therefore, the influence of the MJO on the entrance region of the AEJ will be a significant focus throughout our study. The upstream trigger is necessary since the weak instability and the short length of the AEJ cause the jet alone to be insufficient in supporting observed wave growth (Thorncroft et al. 2008). Strong shear and potential vorticity reversals over an extended region near the AEJ are two conditions that produce stronger AEW responses (Leroux and Hall 2009).

This study hypothesizes that modulation of convection upstream of the AEJ by the MJO may be a key mechanism for producing intraseasonal AEW and convective variability in the West African monsoon. Of particular interest is how moisture and eddy kinetic energy (EKE) vary on MJO timescales in the initiation region and over the greater West African monsoon region.

2. DATA AND METHODOLOGY

Most of the fields analyzed in this study are from the European Centre for Medium-Range Weather Forecasts (ECMWF) interim reanalysis (ERA-I) dataset. The Cloud Archive User Service (CLAUS) brightness temperature (T_B) dataset is utilized as a proxy for convective activity. The CLAUS dataset allows for an excellent representation of convective variability in tropical north Africa, given that important topographically-forced convective features may not be well-represented by coarser resolution datasets. Analysis is performed on daily fields from 1989 to 2005.

To isolate how certain fields are modulated by the MJO, the seasonal cycle is removed and data is filtered to intraseasonal timescales via a linear non-recursive digital bandpass filter with half-power points at 30 and 90 days. Some fields are also spatially-filtered by zonal wavenumber as a means to analyze the modulation of tropical north African fields via eastward- and westward-propagating teleconnected signals from the Indo-Pacific warm pool. Since the teleconnected wave responses are concentrated at low zonal wavenumbers, data is filtered to include wavenumbers 0 to 10 for eastward-propagating disturbances, including Kelvin waves, and wavenumbers -1 to -10 for westward-propagating disturbances, including Rossby waves.

Boreal summer (1 June-30 September) composites that describe the evolution of an MJO lifecycle are constructed based on an index derived from empirical orthogonal functions (EOFs). This “MJO index” entrains daily information about MJO amplitude and phase (see

Alaka and Maloney 2012). The MJO cycle is split into eight phases of equal angular extent, with each phase representing enhanced MJO activity at a particular part of the world. Phase 1 represents the onset of MJO convection in the Indian Ocean. A Student's *t*-test at the 90% confidence interval is performed on composites created from the MJO index to discern whether or not the low amplitude anomalies over tropical North Africa are significant.

3. INTRASEASONAL VARIABILITY IN N. AFRICA

To properly identify the teleconnections between the MJO and AEW initiation, the intraseasonal variability of East Africa is first diagnosed through T_B, low-level EKE, total precipitable water (TPW) and apparent heat source (Q_1) profiles.

The intraseasonal variability of T_B and low-level winds in boreal summer (Fig. 1) reveals that tropical North Africa is convectively enhanced in Phase 1, or when the MJO initiates in the Indian Ocean. With widespread, significant and negative 30-90 day $T_B{}'$ over much of tropical North Africa, Phase 1 will be referred to as the "wet" MJO phase in this region. Significant negative intraseasonal $T_B{}'$ first appear near the Darfur Mountains and Ethiopian Highlands in East Africa by Phase 7. This region may be important for detecting precursors to AEWs that seed the AEJ, and, as a result, we refer to it as the "trigger region" and mark it with a box (10.5°N-24°N, 16.5°E-37.5°E). MJO $T_B{}'$ have about 40-50% of the amplitude of total intraseasonal $T_B{}'$ in the trigger region. Phase 5 will be referred to as the "dry" MJO phase since significant positive 30-90 day $T_B{}'$ are observed over tropical North Africa. Analysis will be limited to the wet MJO phase since the dry MJO phase is generally equal and opposite.

Evidence for increased convection near the AEJ entrance prior to the wet MJO phase is provided by 700 hPa EKE (Fig. 2), TPW (Fig. 3) and apparent heat source (not shown). In Phase 8, or before the wet MJO phase, enhanced wave activity and significant positive column moisture anomalies are observed in the trigger region. Fig. 2 suggests that widespread West African EKE anomalies (e.g. Phase 1) originate upstream in the trigger region (e.g. Phase 8), hinting that a modulation of East Africa by the MJO is important to downstream AEWs. Although intraseasonal TPW does not vary much over West Africa, column moisture anomalies exceed 1 mm in the trigger region prior to the wet MJO phase. Weak TPW anomalies over West Africa suggest the importance of moistening the trigger region.

The apparent heat source (Q_1) is used to diagnose the intraseasonal variability of convective heating profiles in the trigger region (not shown). Q_1 is given in Alaka and Maloney (2012). Above 800 hPa, the mean heating profile is weakly stratiform, with slight cooling below the AEJ (-0.1 K day^{-1}) and heating above the AEJ (+0.5 K day^{-1}). A stratiform heating profile induces a strong heating gradient across the AEJ, which produces

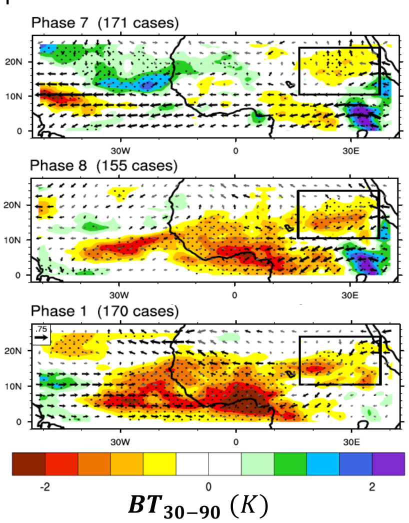

Figure 1. MJO phase composites of 30-90 day variability over tropical north Africa from June to September. 30-90 day CLAUS T_B anomalies (shading) and 30-90 day ERA-I 850 hPa vector wind (vectors). T_B anomalies with 90% significance are marked by stippling while vector wind anomalies with 90% significance are black. The trigger region is marked by a box.

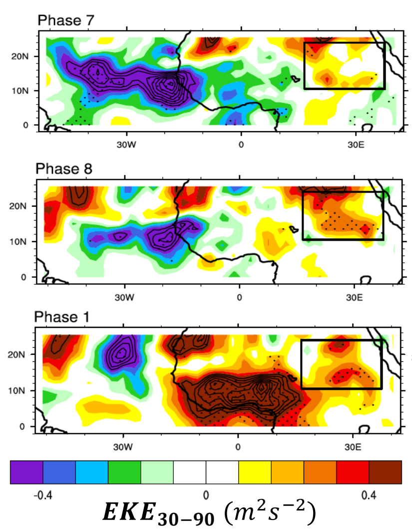

Figure 2. MJO phase composites of 30-90 day ERA-I 700 hPa EKE anomalies for June-September. Stippling represents data that is significant with 90% confidence. Only even phases are included. The trigger region is marked by a box.

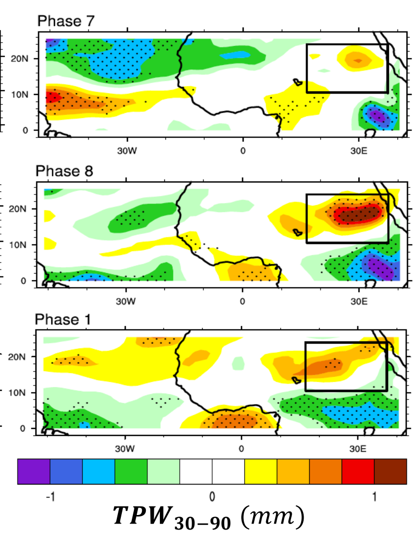

Figure 3. MJO phase composites of 30-90 day ERA-I total precipitable water for June-Sept. Stippling represent data that is significant with 90% confidence. Only even phases are included. The trigger region is marked by a box.

a PV anomaly at the level of the jet. Thorncroft et al. (2008) found that a stratiform heating profile near the AEJ entrance forced a strong wave response. On intraseasonal timescales, an anomalous stratiform heating profile adds constructively to the mean heating profile in Phase 7, while an anomalous shallow heating profile adds destructively to the mean heating profile in Phase 3 (not shown).

4. LARGE-SCALE EQUATORIAL WAVE TELECONNECTIONS

The intraseasonal variability of the trigger region is modulated by equatorial waves emitted by MJO heating in the Indian Ocean. Specifically, Kelvin and equatorial Rossby waves serve as a bridge between the MJO and the trigger region. An MJO heating anomaly produces a coupled Rossby-Kelvin wave response (e.g., Gill 1980) and a radiating Kelvin wave response away from MJO heating. Anomalous upper-tropospheric winds are used to verify the role of MJO-induced equatorial waves for affecting the flow in the trigger region. Links between equatorial waves and thermodynamic/dynamic modulation of large-scale conditions in the trigger region will be used to diagnose how the MJO actually triggers convective variability in the trigger region.

Upon filtering ERA-I 30-90 day 200 hPa vector wind anomalies for eastward-propagating disturbances, Kelvin waves are observed propagating from MJO heating in the Indo-Pacific warm pool to Africa (not shown). In Phase 5, the suppression of MJO heating spawns upper-tropospheric anomalous easterlies. By Phase 1, upper-level easterlies associated with decoupled Kelvin waves arrive at the African coast, where fields in the trigger region may be modulated during the wet MJO phase.

Rossby waves are examined by filtering ERA-I 30-90 day 300 hPa vector wind anomalies for westward-propagating disturbances (not shown). A cyclonic, upper-level Rossby gyre is identified over Tibet/India in Phase 5, or when MJO convection is reduced in the Indian Ocean. Westward propagation into North Africa is apparent by Phase 7 by following significant upper-level westerly anomalies just north of the equator (e.g., the south side of the gyre). Rossby wave signatures arrive in the trigger region two phases, or ~10 days, in advance of Kelvin wave anomalies. The disparate arrival times in the trigger region further suggests that Kelvin and Rossby waves modulate the trigger region in different ways.

5. MODULATION OF THE TRIGGER REGION

This section analyzes the relationship between intraseasonal variability in the trigger region (Section 3) and large-scale equatorial wave teleconnections (Section 4). Specifically, equatorial waves are believed to modulate precursors to AEWs in the trigger region prior to the wet MJO phase by three mechanisms: 1) decreased static stability, 2) AEJ extension, and 3) positive moisture flux.

Negative upper-level air temperature anomalies decrease the static stability, which supports more vigorous deep convection. Since upper-level temperature anomalies may be associated with equatorial waves (Matthews 2004), the modulation of static stability by Kelvin and Rossby waves is examined in the trigger region. The difference in T_{30-90} anomalies between 850 hPa and 400 hPa (e.g., inverse static stability) are averaged in the trigger region for each phase and plotted as the black curve in Fig. 4. Importantly, the static stability decreases in Phases 7 and 8, which primes the trigger region for convection (see Fig. 1). If 400 hPa T_{30-90} anomalies are filtered by zonal wavenumber, eastward-propagating disturbances contribute the most to this reduction in static stability prior to the wet MJO phase. Specifically, a warm Kelvin wave moving along the equator induces off-equatorial temperature anomalies of opposite sign. The static stability mechanism requires further study.

The AEJ is important to the propagation of AEW precursors toward West Africa. Intraseasonal variability of the AEJ in the trigger region is examined through 30-90 day ERA-I 650 hPa zonal wind (e.g., blue curve in Fig. 4). Prior to the wet MJO phase, the 650 hPa zonal wind becomes anomalously easterly in the trigger region, which suggests that the AEJ has extended into (or is at least stronger) in this region. An extension of the AEJ: 1) increases the number of precursor disturbances that enter the jet, 2) enhances energy conversions, and 3) increases residence in the jet. Filtering by zonal wavenumber suggests that Kelvin-like waves explain most of the AEJ variability.

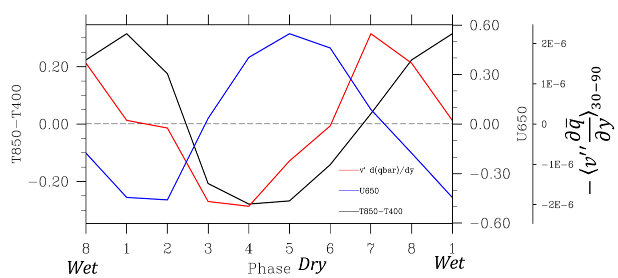

Figure 4. MJO lifecycle for three AEW initiation mechanisms proposed by Alaka and Maloney (2012), averaged in the trigger region. Plotted is meridional moisture advection (red), the anomalous 650 hPa zonal wind, or AEJ length (blue), and the anomalous temperature difference between 850 hPa and 400 hPa, or instability (black). The inverse of the black curve can be interpreted as static stability. The wet and dry MJO phases are labeled. All terms are 30-90-day bandpass filtered.

The vertically-integrated moisture budget, which is examined to assess the moistening in the trigger region prior to the wet MJO phase, is given by:

$$\langle\frac{\partial q}{\partial t}\rangle = -\langle u\frac{\partial q}{\partial x}\rangle - \langle v\frac{\partial q}{\partial y}\rangle - \langle q\nabla\cdot\vec{v}\rangle + E - P - R, \quad (1)$$

where q is the specific humidity, E represents the surface evaporation, P represents precipitation, and R is the residual. (1) was computed using ERA-I fields and vertical integration was conducted from the surface to 200 hPa. The terms in (1) are averaged in the trigger region by MJO phase and compared in Fig. 5. Meridional moisture advection is the dominant moistening process in the trigger region prior to the wet MJO phase (Phases 5-7). Analysis of a linearized meridional moisture advection budget (not shown) suggests that $-\langle v''\frac{\partial\bar{q}}{\partial y}\rangle_{30-90}$ and $-\langle\bar{v}\frac{\partial q''}{\partial y}\rangle_{30-90}$ appear to dominate the meridional advection anomalies. The low-level flow (Fig. 1) suggests anomalous southerly flow in the trigger region centered near 20°N prior to the wet MJO phase (e.g., Phase 7), which emphasizes the importance of $-\langle v''\frac{\partial\bar{q}}{\partial y}\rangle_{30-90}$. Further, $-\langle\bar{v}\frac{\partial q''}{\partial y}\rangle_{30-90}$ appears to be associated with decay of existing moisture anomalies in the trigger region through advection by the mean meridional wind. After filtering the meridional moisture flux terms by zonal wavenumber, it is unclear if Kelvin or Rossby waves have a larger contribution. Kelvin waves may flux moisture from the Gulf of Guinea toward the trigger region, and meridional wind anomalies are likely due to Rossby waves propagating through tropical North Africa from the Indian Ocean (Janicot et al. 2009).

6. CONCLUSION

This study provides evidence that the MJO modulates convective precursor disturbances in East Africa. This sensitive area, known as the "trigger region", exhibits significant convection, moisture, and EKE anomalies prior to maximized convection and wave activity in West Africa. Prior to the wet MJO phase, an anomalous stratiform heating profile adds constructively to the mean heating profile in the trigger region. With evidence of MJO-emitted equatorial waves propagating into tropical North Africa, three mechanisms are identified by which the MJO primes the trigger region for convection: 1) static stability reduction, 2) AEJ extension, and 3) positive moisture flux. Kelvin waves dominate the first two mechanisms, and may even have a significant role in moisture flux. The role of Rossby waves is limited to meridional moisture flux, but this mechanism may be most important. Further analysis of the EKE and eddy-available potential energy budgets is required to understand how these mechanisms vary energy conversions that are important for AEW growth.

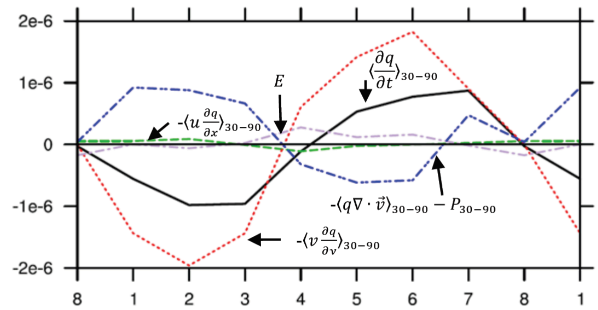

Figure 5. Phase vs. pressure plot of vertically-integrated 30-90 day ERA-I moisture budget term anomalies for June-September in the trigger region. Terms include moisture tendency (black solid), zonal moisture advection (green dashed), meridional moisture advection (red dotted), moisture convergence minus precipitation (blue double dot-dashed), and evaporation (grey dot-dashed).

REFERENCES

Alaka Jr., G. J., and E. D. Maloney, 2011: The Influence of the MJO on Upstream Precursors to African Easterly Waves. J. Climate, in press.

Carlson, T. N., 1969b: Synoptic histories of three African disturbances that developed into Atlantic hurricanes. Mon. Wea. Rev., 97, 256–276.

Gill, A. E., 1980: Some simple solutions for heat-induced tropical circulation. Q. J. R. Meteorol. Soc., 106, 447–462.

Hall, N. M. J., G. N. Kiladis, and C. D. Thorncroft, 2006: Three-dimensional structure of African easterly waves. Part II: Dynamical modes. *J. Atmos. Sci.,* **63**, 2231**–** 2245.

Janicot, S., and Coauthors, 2009: Dynamics of the West African Monsoon. Part IV: Analysis of 25–90-Day Variability of Convection and the Role of the Indian Monsoon. J. Climate, 22, 1541–1565.

Leroux, S., and N. M. J. Hall, 2009: On the Relationship between African Easterly Waves and the African Easterly Jet. J. Atmos. Sci., 66, 2303–2316.

Matthews, A. J., 2004: Intraseasonal variability over tropical Africa during northern summer. J. Climate, 17, 2427–2440.

Thorncroft, C. D., N. M. J. Hall, and G. N. Kiladis, 2008: Three dimensional structure and dynamics of African easterly waves. Part III: Genesis, J. Atmos. Sci., 65, 3596–3607.